Microwave scattered and absorbed powers by a multilayered zero-index anisotropic metamaterial-semiconductor cylinder

Liudmila Nickelson[1] and Juozas Bucinskas[2]

[1]State Research Institute Center for Physical Sciences and Technology, Vilnius, Lithuania
[2]Faculty of Physics, Vilnius University, Sauletekio 9, LT-10222, Vilnius, Lithuania
*corresponding author, E-mail: lucynickelson@gmail.com

Abstract

We present here dependencies of scattered and absorbed powers of incident perpendicularly and parallel polarized microwaves by a multilayered cylinder. We consider here the normal (angle $\theta=90^0$) and oblique (angles $\theta=60^0$, 30^0, 5^0) incidence of microwave on the cylinder. The one consists of a glass core that is coated by the six anisotropic metamaterial and lossy *n*-Si semiconductor alternative layers. Here is presented characteristics of cylinder with the semiconductor external layer. The dispersion dependency of *n*-Si losses was taken into account. The metamaterial is a uniaxial anisotropic medium with the electric and magnetic plasma resonances in the frequency range from 1 till 4 GHz. The anisotropic metamaterial can include the constitutive parameters equal to zero. The multilayered cylinder has the external radius equal to 2 mm. The glass core has a radius equal to 0.5 mm. The thickness of all layers is the same. We have compared the scattered and absorbed power dependencies on the microwave polarization, the angle of microwave incidence (the normal and oblique directions of the incidence to the z-axis) and the *n*-Si specific resistivity. We discovered specific dependencies of scattered and absorbed powers on the parameters.

1. Introduction

The stream of articles devoted to the study of metamaterial scattering (reflecting) structures points that there is a need for development devices possessing unique characteristics. Many applications in modern technologies require the use of special materials with a strong electromagnetic (EM) response. The properties of special composite materials can be strikingly different from the properties of the constituent materials [1]. A composite material can be formed by compounding layers of two or more materials. The resulting composite material has more useful applications than the constituent materials alone. Advanced composite materials can achieve some novel superior properties, for example, electro-optic ones [2], excellent microwave absorption [3], ensure EM compatibility and immunity (insusceptibility) [4]. The multilayer shielding structures with both absorbing and reflecting composite layers are studied in [4].

The importance of diffraction problems for scattering structures made from special composites are based on their great practical utility for many applications, such as reflector antennas, the analysis of structures in the open space, electromagnetic defence of structures, high frequency telecommunications and invisibility cloaks technology [5-11]. The algorithm for exploring the scattering properties of single isotropic and bi-isotropic metamaterial cylinders is proposed in [5]. The enhanced resonant scattering and focusing properties were found in the last article. The full-wave EM scattering theory to study the scattering from infinitely long cylinders with cylindrically anisotropic coatings is given in [6].

The challenging new phenomena are usually discovered when composites contain metamaterials with very low, very large, or negative constitutive parameters. At the moment is an increased interest to the zero-index metamaterials. The metamaterials are attractive due to their unconventional constitutive parameters and different anomalous effects. Zero-index metamaterial may have the epsilon-near-zero (ENZ) or (and) mu-near-zero (MNZ) at some frequencies. Zero - index metamaterials are strongly dispersive media [7-11].

Here we give dependencies of total scattered and absorbed microwave powers of infinite multilayered glass-metamaterial-semiconductor cylinder on the frequency range. The metamaterial is qualified by the tensors of permittivity and permeability. The tensor's components are equal to zero at certain frequencies and the matter can be a zero-index metamaterial.

2. Problem formulation and parameters

In present article we demonstrate our calculation results that based on the rigorous electrodynamical solution of diffraction problem about the microwave scattering by an infinite multilayered cylinder. The solution of Maxwell's equations for the multilayer cylinder was carried out by the partial area method [12-14]. The central core of multilayered cylinder made of glass material. The glass core is coated by a sandwich semiconductor-metamaterial cover. The multilayered cylinder consists of seven concentric surfaces with radii R_j, j=1, 2,..., N (Fig. 1). The every j-th region is filled with a material having the permittivity ε_j and the permeability μ_j. Numbering of layers is going from outside layer to the inner one. Thus R_1 is the outside radius of the cylinder. In our calculations N = 7, i.e. the glass core with radius R_7 is coated with 6 layers of metamaterial and *n*-Si alternately. The radius of glass core is R_7=0.5 mm. The first layer that coated the glass core is a metamaterial layer. The thickness of every layer is equal to 0.25 mm and the outer radius of the multilayered cylindrical structure is R_1=2 mm.

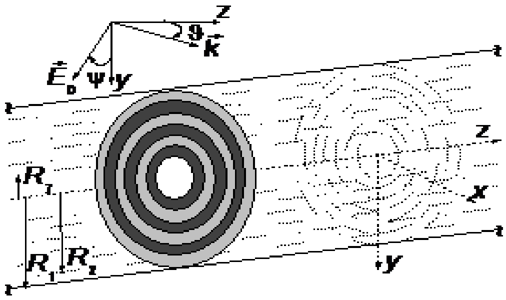

Figure 1: *N*-layered glass-anisotropic metamaterial-semiconductor cylinder model and designations.

As it is known, a semiconductor material with some relatively small specific resistivity is the dispersive lossy material. The imaginary part of semiconductor permittivity Im(ε_s) depends on the operating frequency f and the semiconductor material specific resistivity ρ. The *n*-Si permittivity ε_s is determined by the expression:

$$\varepsilon_s = 11.8 - \mathrm{i}/(\omega\varepsilon_0\rho), \qquad (1)$$

where $\omega = 2\pi f$ is an angular frequency of incident microwave, ε_0 is the electric constant. The semiconductor losses depend on the frequency and this fact strongly affects on the absorbed power into semiconductor layers. The glass and the *n*-Si permeabilities are equal to $\mu_g = \mu_s = 1$.
The incident plane harmonic monochromatic microwave

$$\boldsymbol{E}^{in} = \boldsymbol{E_0}\exp\left(\mathrm{i}(\omega t - \sqrt{\varepsilon\mu}\,\boldsymbol{kr})\right) \qquad (2)$$

propagates in the plane $x0z$ and the direction of microwave propagation describes by an angle θ between the z-axis and the wave vector $\boldsymbol{k}$ (Fig. 1). Here $\boldsymbol{E_0}$ is the amplitude of the electric field of an incident microwave. The vector $\boldsymbol{E_0}$ determines the polarization of the incident microwave. The direction of vector $\boldsymbol{E_0}$ defined by the angle ψ that is between the vector $\boldsymbol{E_0}$ and the y-axis. The EM wave has the parallel polarization when the angle ψ is equal to 90^o. The EM wave has the perpendicular polarization when ψ is equal to 0^o. The module of the amplitude of incident microwave $|\boldsymbol{E_0}|$=1. Here $(\vec{n}_z\vec{k}) = \cos\theta$ and $(\boldsymbol{E_0}\ \boldsymbol{n_y}) = \cos\psi$, $\boldsymbol{k} = k_x \boldsymbol{n_x} + k_z \boldsymbol{n_z}$, where $\boldsymbol{n_x}$, $\boldsymbol{n_y}$, $\boldsymbol{n_z}$ are the unit vectors. The cylinder is placed in an air medium with the permittivity and the permeability $\varepsilon=\mu=1$. Boundary conditions on all surfaces separating different media are the standard ones. The equality of tangent components of the electric and magnetic fields on the glass- metamaterial, every metamaterial–semiconductor, as well as the semiconductor–air surfaces are required [12].

3. Results and discussions

The computer program for calculations has created in FORTRAN language. Our computer program allows take into account a large material attenuation [12-14]. Here the constitutive parameters of the uniaxial electrically and magnetically anisotropic metamaterial were taken from the article [15]. In the last article was considered an anisotropic lossless metamaterial slab. For this reason there were given only the real parts of the permittivity $\varepsilon_{r,ij}$=(ε_{xx}, ε_{xx}, ε_{zz}) and permeability $\mu_{r,ij}$=(μ_{xx}, μ_{xx}, μ_{zz}) tensor components. The tensor components of the relative permittivity and the relative permeability are described by following formulae [15]:

$$\varepsilon_{xx}=1-\omega^2_{epxx}/\omega^2, \qquad \varepsilon_{zz}=1-\omega^2_{epzz}/\omega^2, \qquad (3)$$

$$\mu_{xx}=1-\omega^2_{mpxx}/\omega^2, \qquad \mu_{zz}=1-\omega^2_{mpzz}/\omega^2. \qquad (4)$$

The values of tensors' components ε_{xx}, ε_{zz},. μ_{xx}, μ_{zz} become equal to zero at the operating frequency f equal to the metamaterial electric f_{epxx}=3.46 GHz, f_{epzz}=2.5 GHz and magnetic f_{mpxx}=2.45 GHz, f_{mpzz}=2 GHz plasma resonance frequencies. The core of our multilayered cylinder is made of acrylic glass with the permittivity ε_{glass}=3.8- i0.0005. The semiconductor layers were made of electronic type silicon (*n*-Si) with the specific resistivities ρ= 100, 30, 10 Ω·m. We take into account the dispersion of semiconductor by formula (1). The calculations of the total scattered W^s and total absorbed W^a powers were fulfilled using method of article [12]. Under the term "total power" we mean the sum power (scattered or absorbed) by the all layers and the core of multilayered cylinder. The dependencies of total W^s and W^a powers that are normalized to the unit length of multilayered cylinder and through one oscillation period are presented in Figs 2– 9. Dependencies for the incident perpendicular polarized microwave are shown in Figs 2(a)–9(a). Dependencies for the incident parallel polarized microwave are given in Figs 2(b)– 9(b). Designations in Figs 2–9 correspond: curve 1 (line with empty squares) for ρ=100 Ω·m; curve 2 (line with empty circulars) for ρ=30 Ω·m; curve 3 (line with empty triangulars) for ρ= 10 Ω·m. We explored the dependencies from 1 till 40 GHz. Here we present our calculations in the most interesting microwave range where happened uniaxial anisotropic metamaterial resonances from 1 till 4 GHz. We would like to pay your attention that the upper part of the resonance peaks has been cut to see better the character of dependencies along of the metamaterial resonance frequencies (Figs 2–9).

3.1 Scattered power in the anisotropic metamaterial resonances' frequency range

The scattered power W^s presented for three values of the *n*-Si specific resistivity ρ at two polarizations and four angles θ=90^o (Fig. 2), θ=60^o (Fig. 3), θ=30^o (Fig. 4) and θ=5^o (Fig. 5) of microwave incidence.

The specific resistivity ρ varies within ten times in our calculations. The imaginary part of the semiconductor permittivities Im (ε_s) changes from 0.18 till 1.8 at f =1 GHz. The scattered power depends weakly on the specific resistivity (Figs 2–5) in spite of the large Im (ε_s).
Analysis of the scattered power dependencies of multilayered cylinder shows that there are strongly expressed resonance peaks. We see that these peaks are on other frequencies than the anisotropic metamaterial resonances that is calculated by formulae (3) and (4) but all resonances are in the same frequency range between 1 and 4 GHz. If instead of uniaxial anisotropic layers 2, 4, 6 in the frequency range from 1 GHZ till 4 GHz are some

isotropic medium, then scattered and absorbed powers have not any resonance picks for the both polarizations.

The comparison of scattered powers for the microwave perpendicular (Fig. 2(a)) and parallel (Fig. 2(b)) polarizations at θ=90^{o} shows the significantly different features the ones. We see three W^{s} resonances for both microwave polarizations. The central resonance frequencies of the W^{s} resonances for the perpendicular polarized microwave are observed at frequencies equal to 2.28, 2.92 and 3.26 GHz. The central resonance frequencies of W^{s} resonances for the parallel polarized microwave are at f= 1.2, 2.13 and 2.4 GHz.

The scattered power resonances are very narrow for the incident microwave with the parallel polarization. The last properties can be useful for working out of precision-sensor devices.

The comparison of Figs 2(a)–5(a) shows that the smaller the angle θ is the more complex the W^{s} resonance distributions are in the frequencies between 1 and 4 GHz. We see that the values of scattered power minima decrease with decreasing of angle θ. This decrease is the particularly noticeable at frequencies between 3 and 4 GHz.

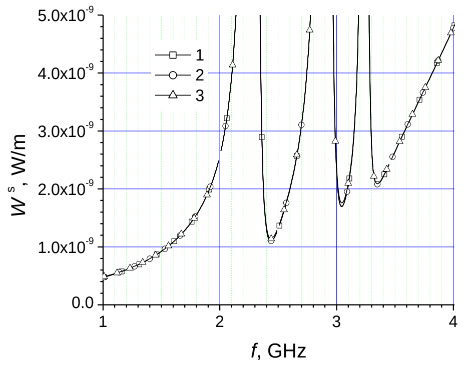

(a)

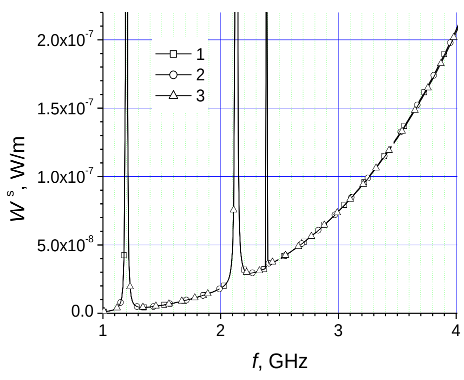

(b)

Figure 2: Scattered power of multilayered cylinder on the frequency of incident (a) − perpendicular and (b) − parallel polarized microwave at θ=90^{0}.

There are six resonances of scattered power for both microwave polarizations at the oblique incidence of microwave. The central resonance frequencies of perpendicular and parallel polarized microwaves are at frequencies equal to 1.2, 2.13, 2.28, 2.4, 2.92 and 3.26 GHz when θ=60^{0}, 30^{0} and 5^{0} (Figs 3-5).

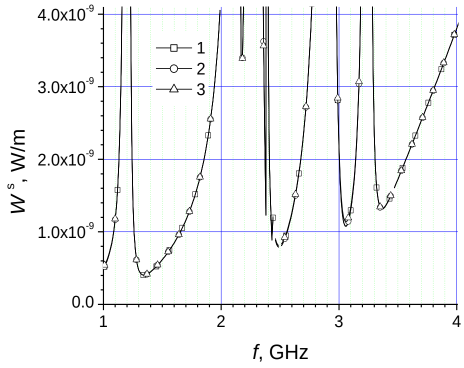

(a)

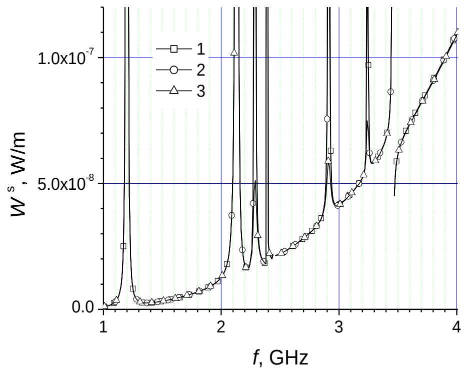

(b)

Figure 3: Scattered power of multilayered cylinder on the frequency of incident (a) − perpendicular and (b) − parallel polarized microwave at θ=60^{0}.

We can see that the central resonance frequencies at the oblique microwave incidence for the every of polarizations (Figs 3-5) are equal to the sum of all resonance frequencies at the normal microwave incidence (Fig. 2). It is possible to determinate the value θ, i.e. the location of a microwave radiation source, thanks to the knowledge of scattered power minimum values.

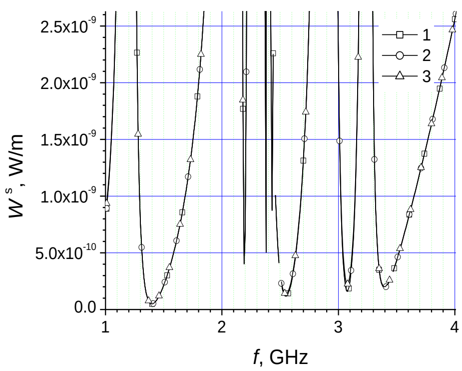

(a)

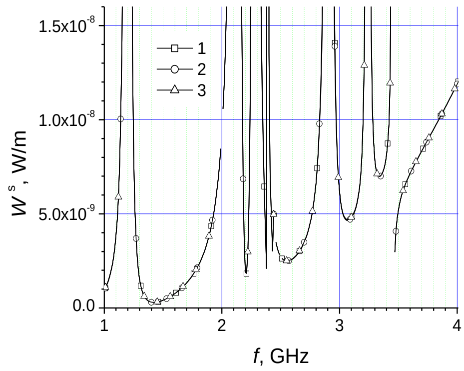

(b)

Figure 4: Scattered power of multilayered cylinder on the frequency on the frequency of incident (a) − perpendicular and (b) − parallel polarized microwave at θ=30^0.

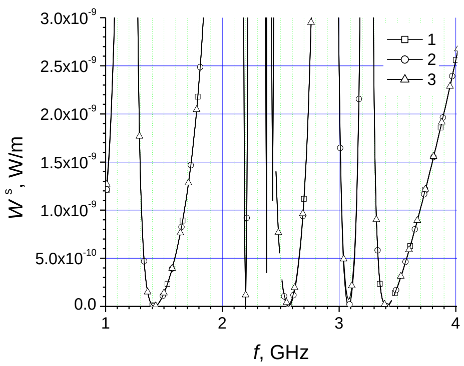

(a)

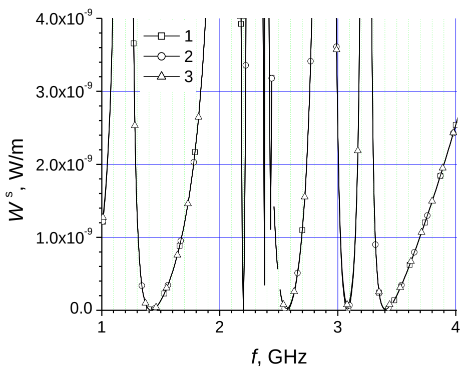

(b)

Figure 5: Scattered power of multilayered cylinder on the frequency of incident (a) − perpendicular and (b) − parallel polarized microwave at θ=5^0.

The less θ is the smaller scattered powers are at the certain frequencies. As an example, the scattered power is approximately zero and the cylinder become invisible at frequencies equal to 3.1 and 3.4 GHz when θ=5^o (Fig. 5).

We would like to pay your attention on an interesting detail. The scattered power distributions on the frequency for the perpendicular and parallel polarizations are approximately similar at small angles θ.

This can be explained by the fact that the configuration of falling EM fields becomes identical. We see that the W^s resonance pictures for both microwave polarizations are very similarly at θ=5^0 (Fig 6 (a, b)).

3.2 Absorbed power in the anisotropic metamaterial resonances' frequency range

The absorbed power W^a presented for three values of the *n*-Si specific resistivity ρ at two polarizations of incident microwave and four angles of incidence θ =90^o (Fig. 6), θ =60^o (Fig. 7), θ =30^o (Fig. 8) and θ =5^o (Fig. 9).

We see that W^a substantially depends on the specific resistivity of semiconductor material. This dependence is fairly large in the frequency intervals between the W^a resonance frequencies. As we explored dependencies till 40 GHz we can remark that W^a dependence on ρ is also strong between 5 and 40 GHz. We see in Fig. 6(a) the smaller specific resistivity the wider resonance curve for the perpendicular polarized microwave. The comparison of absorbed power for both polarizations when θ =90^o shows that there is the noticeable difference in their distributions. The central resonance frequencies are 2.3, 2.9 3.25 GHz for the incident microwave with the perpendicular polarization and 1.2, 2.1, 2.4 GHz for the incident microwave with the parallel polarization. The W^a resonance frequencies do not move with the changing of value ρ for both polarizations. All W^a resonance curves are very narrow for the parallel polarized microwave at θ=90^o. The absorbed power for the microwave with the parallel polarization depends stronger on the *n*-Si specific resistivity than for microwave with the perpendicular one at the frequency intervals between W^a resonance frequencies (see Fig. 6(a, b)). As an example, frequencies can be between 1.4 and 1.9 GHz or 2.5 and 2.8 GHz. Absorbed power dependencies Fig. 6(b) can be used for the precision determination of semiconductor specific resistivity of multilayered cylinder when the incident parallel polarized microwave impinges at θ=90^0.

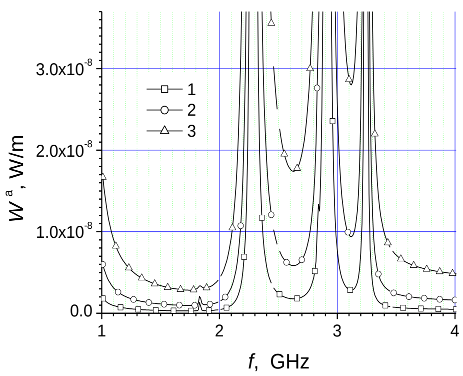

(a)

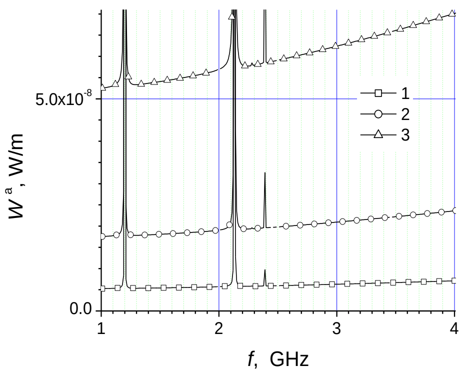

(b)

Figure 6: Absorbed power of multilayered cylinder on the frequency of incident (a) − perpendicular and (b) − parallel polarized microwave at θ=90^0.

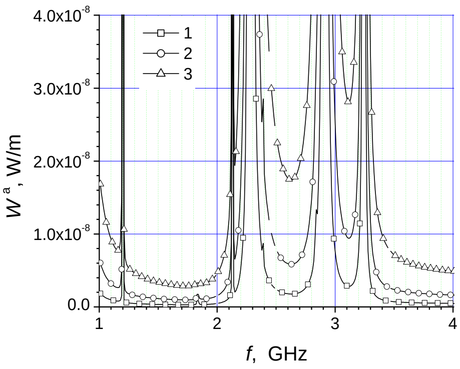

(a)

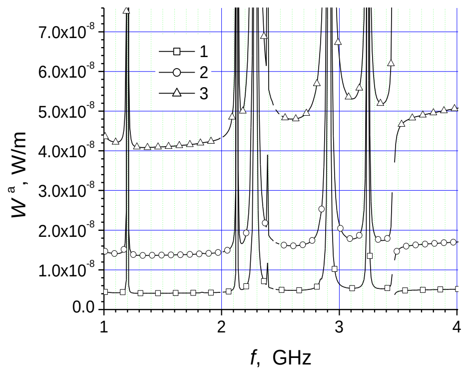

(b)

Figure 7: Absorbed power of multilayered cylinder on the frequency of incident (a) − perpendicular and (b) − parallel polarized microwave at θ=60^0.

In this case we have to know the incident microwave polarization, angle θ, main parameters of other cylinder materials and geometrical sizes.

In Fig. 6 are three resonances while in Figs 7−9 are six resonances. The values of W^a resonance frequencies match with the W^s resonance frequencies.

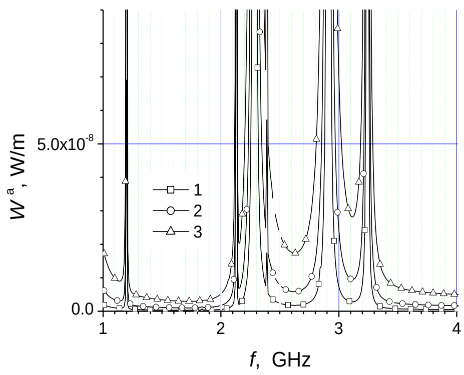

(a)

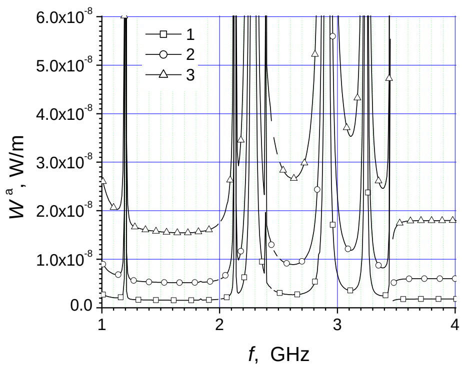

(b)

Figure 8: Absorbed power of multilayered cylinder on the frequency of incident (a) − perpendicular and (b) − parallel polarized microwave at θ=30^0.

The larger value of specific resistivity is the wider resonance curves are for the perpendicular polarized microwave at different angles θ (Figs 7(a), 8(a)). The location of resonance frequencies practically does not depend on the semiconductor specific resistivity for the parallel polarized microwave (Figs 6(b)−9(b).

We can also see that the distribution of absorbed power for both polarizations is similar at the small incident angles, i.e. when $\theta = 5^0$ (Fig. 9(a, b)).

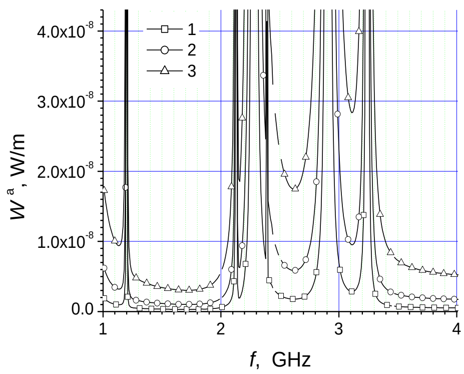

(a)

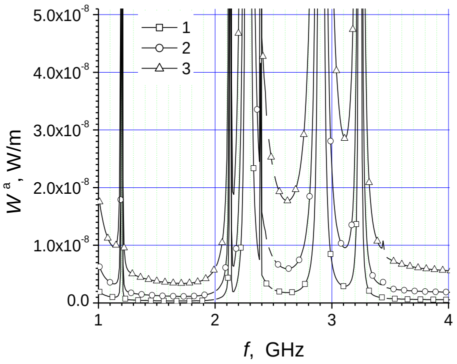

(b)

Figure 9: Absorbed power of multilayered cylinder on the frequency of incident (a) − perpendicular and (b) − parallel polarized microwave at $\theta=5^0$.

The reason of this is the same as for the scattered power (Fig. 5(a, b)), i.e. the incident EM field configurations are similar for both polarizations when θ is small.

4. Conclusions

1. Analyses of scattered and absorbed microwave powers of multilayered cylinder that consists of the glass core coated with six uniaxial anisotropic metamaterial-semiconductor layers is carried out on the base of the rigorous solution of the boundary diffraction problem.
2. Resonances of multilayered metamaterial-semiconductor cylinder are in the same frequency range as resonances of the metamaterial. We can observe three and six resonances of the multilayered cylinder at normal ($\theta=90^0$) and oblique ($\theta=60^0$, 30^0, 5^0) microwave incidence correspondingly instead of four resonances of the uniaxial anisotropic metamaterial.
3. The microwave power dependencies on the *n*-Si specific resistivity, the incident microwave polarization and the incident angle of microwave are implemented.
4. A magnitude of absorbed power is strongly dependent on the *n*-Si material specific resistivity at the frequency intervals between the frequencies of multilayered cylinder resonances. These dependencies are especially strong for parallel polarization at $\theta=60^0$ and 90^0. The dependence on the specific resistivity shows that this multilayered cylindrical structure can be used for creating of microwave semiconductor sensor.
5. There are narrow resonances of the scattered and absorbed powers of parallel polarized microwave at $\theta=90^0$. These resonances can be used for the determination of microwave polarization.

References

[1] G.W. Milton, *The theory of composites*, Cambridge university press, New York, 2002.

[2] R. L. Nelson, R. W. Boyda, Enhanced electro-optic response of layered composite materials, *Applied physics letters* 74: 2417–2419, 1999.

[3] D. Micheli, C. Apollo, R. Pastore, R. Bueno Morles, M. Marchetti, G. Gradoni, Electromagnetic Characterization of Composite Materials and Microwave Absorbing Modeling. *In book: Advances in Nanocomposites - Synthesis, Characterization and Industrial Applications*. ISBN 978-953-307-165-7, InTech, Ch.16: pp. 359–384, 2011.

[4] M. Y. Koledintseva, J. Drewniak, R. DuBroff, K. Rozanov, B. Archambeault, Modeling of shielding composite materials and structures for microwave frequencies, *PIER B* 15: 197–215, 2009.

[5] C. W. Qiu, H.-Y. Yao, S.-N. Burokur, S. Zouhdi, L.-W. Li, Electromagnetic scattering properties in a multilayered metamaterial cylinder, *IEICE Trans. Commun.* E90-B: 2423–2429, 2007.

[6] Y. Ni, L. Gao, C.-W. Qiu, Achieving Invisibility of Homogeneous Cylindrically Anisotropic Cylinders, Plasmonics 5:251–258, 2010.

[7] H. Oraizi, A. Abdolali, N. Vaseghi, Introduction of a New class of materials called double zero media having the real parts of epsilon and mu equal to zero, *PIERS Proceedings*, Moscow, Russia, pp. 348–350, 2009.

[8] H. Zhou, Z. Pei, S. Qu, S. Zhang, and J. Wang, A planar zero-index metamaterial for directive emission, *J. of Electromagn. Waves and Appl.* 23: 953–962, 2009.

[9] N. M. Litchinitser, A. I. Maimistov, I. R. Gabitov, R. Z. Sagdeev, V. M. Shalaev, Metamaterials: electromagnetic enhancement directive emission, *Optics Letters* 33: 2350–2352, 2008.

[10] A. Alú, Restoring the physical meaning of metamaterial constitutive parameters, *Physical Review B* 83: 081102-(1–4), 2011.

[11] M. Silveirinha, N. Engheta, Design of matched zero-index metamaterials using nonmagnetic inclusions in epsilon-near-zero media, *Physical Review B* 75: 075119-(1–10), 2007.

[12] J. Bucinskas, L. Nickelson, V. Sugurovas, Microwave diffraction characteristic analysis of 2D multilayered uniaxial anisotropic cylinder, *Progress In Electromagn. Research*, PIER109: 175–190, 2010.

[13] J. Bucinskas, L. Nickelson, V. Sugurovas, Microwave scattering and absorption by a multilayered lossy metamaterial-glass cylinder, *Progress In Electromagn. Research*, PIER105: 103–118, 2010.

[14] L. Nickelson, J. Bucinskas, Microwave diffraction dependencies of a conductor cylinder coated with twelve glass and semiconductor layers on the *n*-Si specific resistivity. *Electronics and Electrical Engineering*, 115: 47–50, 2011.

[15] S.-H. Liu, C.-H. Liang, W. Ding, L. Chen, W.-T. Pan, Electromagnetic wave propagation through a slab waveguide of uniaxially anisotropic dispersive metamaterial, *Progress In Electromagn. Research*, PIER 76: 467–475, 2007.